

Microscopic sound waves in dense Lennard-Jones fluids

I. M. de Schepper, J. C. van Rijs, A. A. van Well, P. Verkerk, and L. A. de Graaf
Interuniversitair Reactor Instituut, 2629 JB Delft, The Netherlands

C. Bruin

*Laboratorium voor Technische Natuurkunde, Delft University of Technology,
 2600 GA Delft, The Netherlands*

(Received 2 December 1983)

Molecular-dynamics simulations of dense Lennard-Jones-like fluids show new evidence for the existence of sound waves with wavelengths comparable to the size of the atoms. The sound frequency vanishes for a small but finite region of wavelengths as predicted by kinetic theory, and appears to depend mainly on the repulsive part of the interaction potential.

In dense classical monatomic fluids, sound waves with wavelengths λ of the order of the atomic diameter σ were first observed in neutron scattering experiments on liquid rubidium.¹ In these experiments the sound waves manifest themselves as distinct side peaks in the measured dynamic structure factor $S(k, \omega)$, where $\hbar k = 2\pi\hbar/\lambda$ and $\hbar\omega$ denote the transfer of momentum and energy, respectively, from the fluid to the neutrons. Side peaks are absent when $\lambda < \lambda_v \sim 1.5\sigma$, where λ_v is the "visibility limit wavelength." For dense systems of particles interacting through Lennard-Jones types of potentials, molecular-dynamics experiments show distinct side peaks in $S(k, \omega)$ for λ down to $\lambda_v \sim 6\sigma$.² Thus there is direct evidence for the existence of collective excitations with wavelengths larger than, but comparable to, the atomic diameter σ .

On the other hand, it follows from a kinetic theory for a dense fluid of hard spheres³ that $S(k, \omega)$ is dominated by three (extended) hydrodynamic modes, i.e., one heat mode and two sound modes, for λ down to a fraction of σ . Furthermore, it appears that the shape of $S(k, \omega)$ is mainly determined by the heat-mode contribution and that for $\lambda < \lambda_v \sim 6\sigma$ side peaks are absent since the sound-mode contributions are too weak and broad to be distinguished. Recent neutron scattering experiments on liquid argon at a temperature $T = 120$ K and pressure $p = 20$ bars, analyzed on the basis of a least-squares fitting procedure, are consistent with this description of $S(k, \omega)$ in terms of extended heat and sound modes and with such an explanation for the absence of visible side peaks.⁴ It also appeared from these experiments that the extended sound modes, although not directly visible in $S(k, \omega)$, do determine the locations and the heights of the two maxima which are present in the related function $\omega^2 S(k, \omega)$ and, therefore, dominate the shape of this function for λ far below λ_v . In our view, these results from theory and experiment show that λ_v is a limit neither to the existence of sound waves nor to their direct observability.

This point of view allows a study of the dispersion curve $\omega_s(k)$ for values of $k\sigma$ beyond the limit $2\pi\sigma/\lambda_v$, which is about 1 for Lennard-Jones-like fluids and for systems of hard spheres. Thus it was found on the basis of kinetic theory that the sound frequency $\omega_s(k)$ calculated for hard spheres as a function of k vanishes in a small but finite region around $k\sigma \sim 2\pi$, i.e., $\lambda \sim \sigma$.³ Later, the analysis of neutron scattering results for liquid argon at 120 K and 20 bars confirmed this prediction of the existence of such a gap

in the sound dispersion $\omega_s(k)$.⁴

In order to better understand this peculiar feature and how, in particular, it depends on the interparticle potential, we performed molecular-dynamics simulations for three systems with different effective interparticle potentials. The first system is representative for liquid argon at 120 K and 115 bars for which neutron scattering data for $S(k, \omega)$ are available,⁵ whereas the second and third systems are increasingly more representative for a fluid of hard spheres.

We consider the intermediate scattering function $F(k, t)$ and the longitudinal current correlation function $C(k, t)$ which can be conveniently obtained from computer simulations, rather than their Fourier transforms $S(k, \omega)$ and $\omega^2 S(k, \omega)$, which are more directly accessible in neutron scattering experiments. Since both approaches are equivalent, we expect that the heat mode will dominate $F(k, t)$ and the sound modes $C(k, t)$ and that therefore the behavior of all three extended hydrodynamic modes will appear most clearly when $F(k, t)$ and $C(k, t)$ are considered simultaneously. These functions are defined as

$$F(k, t) = \sum_{j,l} \frac{1}{N} \langle \exp\{i\vec{k} \cdot [\vec{r}_j(t) - \vec{r}_l(0)]\} \rangle, \quad (1)$$

$$C(k, t) = \sum_{j,l} \frac{\beta m}{Nk^2} \langle \vec{\nabla}_j(t) \cdot \vec{k} \vec{\nabla}_l(0) \cdot \vec{k} \exp\{i\vec{k} \cdot [\vec{r}_j(t) - \vec{r}_l(0)]\} \rangle, \quad (2)$$

where the brackets denote an equilibrium ensemble average at temperature T and density $n = N/V$, with N the number of particles and V the volume of the system, m the mass of a particle, $\beta = 1/k_B T$ with k_B Boltzmann's constant, and $\vec{r}_j(t)$ and $\vec{\nabla}_j(t)$ denote, respectively, the position and velocity of particle j at time t .

We performed simulations for a three-dimensional system of 256 particles using periodic boundary conditions and a cut-off Lennard-Jones potential $\phi(r, r_c)$ which vanishes for $r \geq r_c$, is continuous at $r = r_c$, and is given by

$$4\epsilon[(\sigma/r)^{12} - (\sigma/r)^6 - (\sigma/r_c)^{12} + (\sigma/r_c)^6]$$

for $r \leq r_c$. We considered three cases. First, $r_c = 2.5\sigma$, reduced density $n\sigma^3 = 0.692$, and reduced temperature $k_B T/\epsilon = 0.97$. This case closely represents a fluid of particles interacting through a Lennard-Jones potential and will be denoted as LJ. In the second and third cases, $r_c = 2^{1/6}\sigma$,

$n\sigma^3 = 0.692$, and $k_B T/\epsilon = 0.97$ and 3.90 , respectively. These systems represent fluids of particles interacting through a purely repulsive potential and are denoted as RLJ. The values of $k_B T/\epsilon$ are such that in case 2 the particles interact mainly through the soft lower part of the potential near $r=r_0$, while in case 3, for $r < r_c$ the steep part ($\sim r^{-12}$) dominates. We followed each system in time up to $100\tau_\sigma$ with an increment of $0.01\tau_\sigma$. Here the time $\tau_\sigma = \frac{1}{2}\sqrt{\beta m} \sigma$ is representative for the time a free particle needs to transverse σ with thermal speed. We obtained $F(k,t)$ from Eq. (1) and $C(k,t)$ from Eq. (2) for $0.88 \leq k\sigma \leq 15$. Errors in $F(k,t)$ and $C(k,t)$ are estimated by repeating each simulation 5 times with different initial configurations.

For the analysis of the computer results we use that, according to kinetic theory, $F(k,t)$ and $C(k,t)$ can be described by an infinite sum of exponentials,³

$$F(k,t) = \sum_{j=-\infty}^{+\infty} A_j(k) e^{-z_j(k)|t|}, \quad (3)$$

$$C(k,t) = -\frac{\beta m}{k^2} \sum_{j=-\infty}^{+\infty} A_j(k) z_j^2(k) e^{-z_j(k)|t|}, \quad (4)$$

where Eq. (4) follows from Eq. (3) since

$$C(k,t) = -(\beta m/k^2)(\partial^2/\partial t^2)F(k,t)$$

[cf. Eqs. (1) and (2)]. The parameters $A_j(k)$ and $z_j(k)$ in Eqs. (3) and (4) can be determined explicitly from kinetic theory but here we use only that A_j and z_j are either real or appear in complex-conjugate pairs and obey sum rules ($l=0, 1, 2, \dots$)

$$\sum_{j=-\infty}^{\infty} A_j(k) [z_j(k)]^l = R_l(k), \quad (5)$$

where $R_0(k) = F(k, 0) = S(k)$ is the static structure factor, $R_1(k) = 0$ and $R_2(k) = -k^2/\beta m$, implying that $C(k, 0) = 1$. Also according to kinetic theory³ only three terms on the right-hand sides of Eqs. (3) and (4) are sufficient to describe $F(k,t)$ and $C(k,t)$ up to $k\sigma \sim 12$. These terms represent the extended heat-mode contribution ($j=0$) and two extended sound-mode contributions ($j = \pm 1$) which are continuous extensions of the heat and sound modes in the hydrodynamic regime (i.e., the regime where $k\sigma \ll 1$) to larger values of $k\sigma$.

In accordance with kinetic theory we find indeed that for

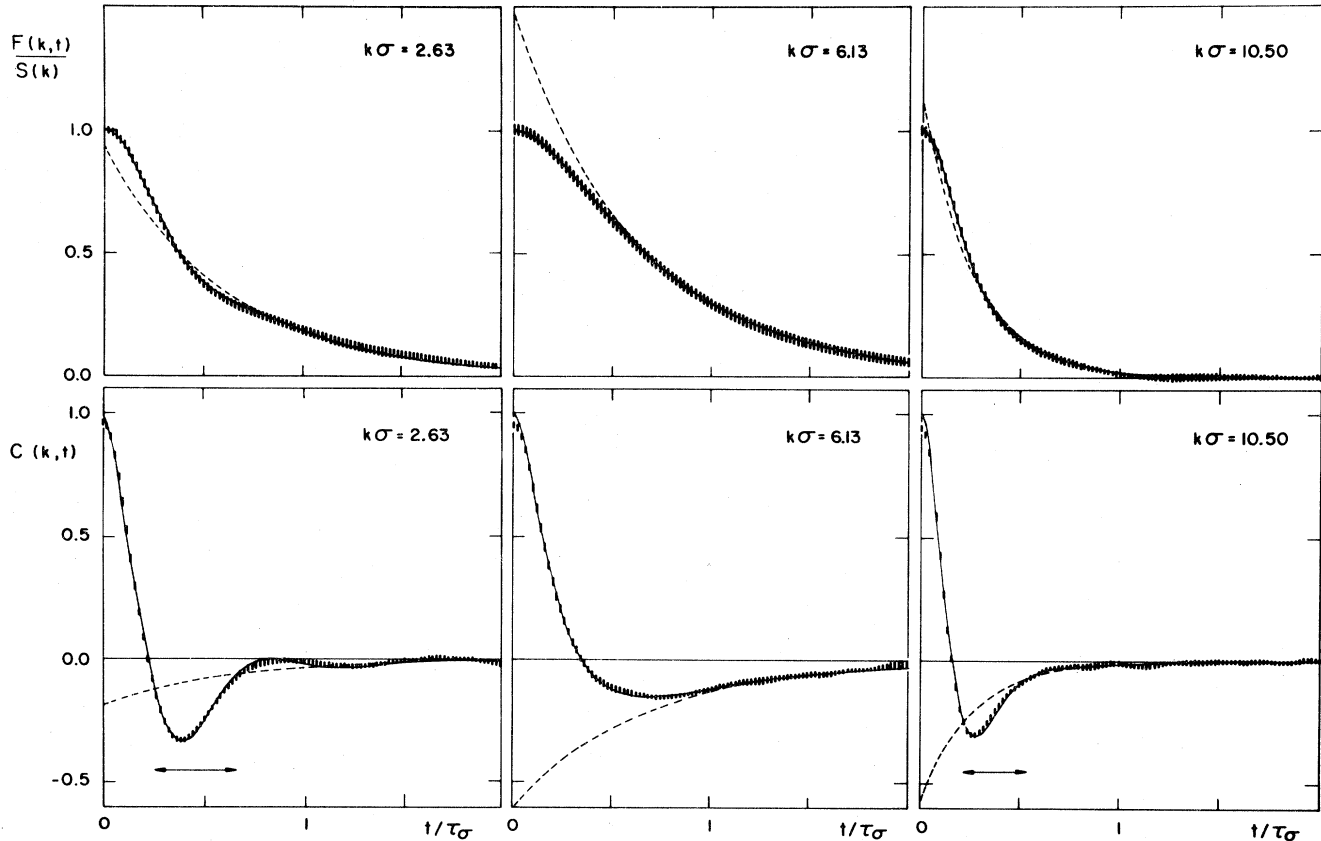


FIG. 1. Molecular-dynamics results (vertical bars) for the intermediate scattering function $F(k,t)$ and the longitudinal current correlation function $C(k,t)$ for a Lennard-Jones system of 256 particles at reduced density $n\sigma^3 = 0.692$ and reduced temperature $k_B T/\epsilon = 0.97$. The unit of time is $\tau_\sigma = \frac{1}{2}\sqrt{\beta m} \sigma$. The sums of the contributions of the three extended hydrodynamic modes, obtained from a least-squares fitting procedure, cf. Eqs. (3) and (4) with $j=0, \pm 1$, are shown as full curves. The separate contributions of the extended heat modes are indicated by dashed curves. The separate sound-mode contributions are equal to the differences of the full and dashed curves. Sound oscillations are indicated by horizontal arrows, whose lengths are $\pi\omega_s(k)^{-1}$, with $\omega_s(k)$ the sound frequency. Note the absence of oscillations at $k\sigma = 6.13$.

all k and for both LJ and RLJ, $F(k,t)$ and $C(k,t)$ can be described by the Eqs. (3) and (4), respectively, with three terms ($j=0 \pm 1$) on the right-hand side. For each k the parameters $A_j(k)$ and $z_j(k)$ are determined from the computer data in a weighted least-squares fitting procedure. The mean-square deviation of the data points from the best-fitted three exponentials is at most 1.5 if we require Eq. (5) to hold exactly for $l=1$ and $l=2$, and slightly smaller if we remove these conditions. We consider these deviations as sufficiently small to justify the interpretation of the simulation data in terms of three extended hydrodynamic modes. For LJ and RLJ and all k the values for $A_0(k)$ and $z_0(k)$ obtained from the fitting procedure are real so that the heat-mode contribution in Eq. (3) and in Eq. (4) decays exponentially in time. For LJ and RLJ and most wave numbers we find complex values for the parameters $A_{\pm 1}(k)$ and $z_{\pm 1}(k)$. For these k values the contribution of the two sound modes oscillates in time with frequency $\omega_s(k) = |\text{Im}z_{\pm 1}(k)|$ and is exponentially damped both for $F(k,t)$ and $C(k,t)$. However, for a few values of k we find for $j = \pm 1$ that $A_j(k)$ and $z_j(k)$ are real and different for $j = +1$ and -1 . In this gap region, $\omega_s(k) = 0$ and the sound-mode contributions in Eqs. (3) and (4) are damped exponentially, just as was found before from kinetic theory for hard spheres and experimentally for liquid argon.

The results for $F(k,t)$ and $C(k,t)$ are shown in Fig. 1 for three representative wave numbers and for the case LJ. In addition, we display the sum of the three exponentials which fit the experiments best [cf. Eqs. (3) and (4)] and which satisfy Eq. (5) exactly for $l=1$ and $l=2$. The separate contribution of the extended heat mode is also indicated. In Fig. 2 we display $\omega_s(k)$ as a function of k for LJ and RLJ. Uncertainties in $\omega_s(k)$ include the values obtained in the fits using either 0, 1, or 2 sum-rule restrictions.⁴ Also shown in Fig. 2 are values of $\omega_s(k)$ for liquid argon at 120 K and 115 bars which were obtained in the same way as described in Ref. 4. We used $\epsilon/k_B = 123$ K and $\sigma = 3.36$ Å (Ref. 6) in order to compare the argon data with the present results.

We conclude the following from our results. (1) The existence of a gap around $k\sigma \sim 2\pi$ appears to be insensitive to the details of the interaction potential and has about the same size for all four systems at the density considered (cf. Fig. 2). Since also a gap in $\omega_s(k)$ is observed in liquid argon at 20 bars (Ref. 4), and since it appears from the kinetic-theory calculations for a dense system of hard spheres, it might well be a general phenomenon for dense classical fluids. We remark that, for reduced wave numbers $k\sigma$ comparable to those considered here, a gap in $\omega_s(k)$ is not found for a hard-sphere fluid at low densities,³ for liquid helium at low temperatures,⁷ for glasses,⁸ or for crystalline solids. The origin of this difference in behavior is not clear at present. (2) $\omega_s(k)$ has about the same shape for the cases LJ and RLJ at the same temperature (cf. Fig. 2). Therefore, $\omega_s(k)$ does not seem to be very sensitive to the attractive part of the interaction potential and is mainly determined by the repulsive part. This dependence is illustrated in Fig. 2 by the decrease of $\omega_s(k)$ below the gap, i.e., for $k\sigma \leq 2\pi$, with increasing steepness of the potential. This behavior is consistent with that predicted by kinetic theory for a hard-sphere fluid and also with results from neutron scattering experiments on liquid rubidium¹ and lead.⁹ For, as noted by Söderström,⁹ the interparticle poten-

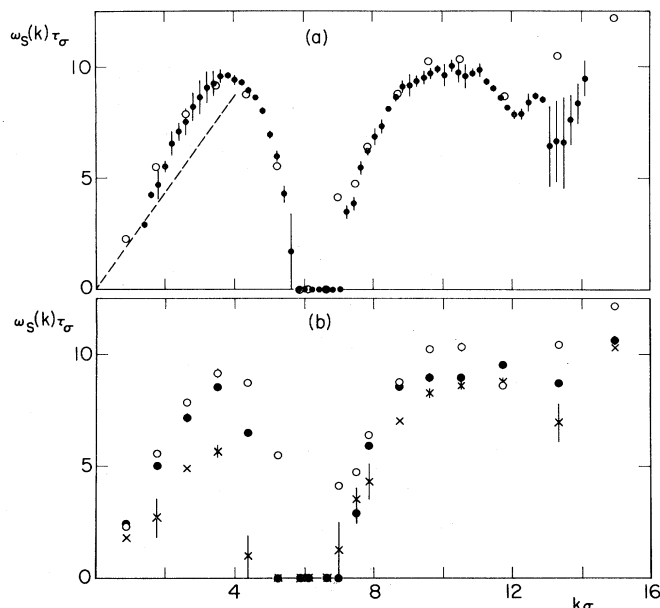


FIG. 2. The sound frequency $\omega_s(k)$ as a function of k for liquid argon at $T = 120$ K and $p = 115$ bars [dots with representative uncertainties in (a)], a Lennard-Jones system at $k_B T/\epsilon = 0.97$ [open circles in (a) and (b)] and for two systems of particles interacting through a repulsive Lennard-Jones potential, with $k_B T/\epsilon = 0.97$ [closed circles in (b)] and with $k_B T/\epsilon = 3.90$ [crosses in (b)], respectively. The density in all cases is $n\sigma^3 = 0.692$. The dashed curve in (a) represents $\omega_s(k) = ck$ with $c = 724$ ms⁻¹, the adiabatic speed of sound for liquid argon. Note for all cases the region around $k\sigma = 2\pi$, where $\omega_s(k) = 0$.

tial for lead is steeper than that for rubidium. (3) In Fig. 1 we clearly see that, as in the hydrodynamic region, the heat mode dominates the shape of $F(k,t)$, while the sound modes dominate that of $C(k,t)$. For $k\sigma = 2.63$ and 10.50 the sound-mode contributions have a visible oscillatory behavior while for $k\sigma = 6.13$ such oscillations are absent. Thus the gap in $\omega_s(k)$ seems to manifest itself directly in $F(k,t)$ and $C(k,t)$ and appears to be responsible for the very smooth forms of these functions for wave numbers around $k\sigma = 2\pi$. We conclude from Fig. 1 that a description in terms of three extended hydrodynamic modes explains quite naturally the shapes of $F(k,t)$ and $C(k,t)$, including the region around $k\sigma = 2\pi$. (4) The values of $\omega_s(k)$ for the case LJ agree with those for argon for $0.88 \leq k\sigma \leq 15$ (cf. Fig. 2). In fact we find that, within the experimental uncertainty, all six parameters $A_j(k)$ and $z_j(k)$ agree for both cases. This implies that also $F(k,t)$ and $C(k,t)$, or equivalently $S(k,\omega)$ and $\omega^2 S(k,\omega)$, are the same for LJ and argon at 115 bars. (5) The present analysis strongly supports the idea that the absence of side peaks in $S(k,\omega)$ does not mean an absence of collective modes. On the contrary, it appears that the neutron spectra are determined by these modes for wavelengths far below the visibility limit wavelength λ_v in $S(k,\omega)$. (6) For $k\sigma < 4$, anomalous dispersion caused by coupling of the hydrodynamic modes is visible both in the neutron scattering results^{4,5} as well as in the present LJ computer simulation results. The density dependence of mode coupling and gap width will be discussed in future publications.

We are grateful to Professor E. G. D. Cohen for many useful discussions and for his stimulating interest.

¹J. R. D. Copley and J. M. Rowe, Phys. Rev. Lett. 32, 49 (1973).

²S. W. Haan, R. D. Mountain, C. S. Hsu, and A. Rahman, Phys. Rev. A 22, 767 (1980).

³I. M. de Schepper and E. G. D. Cohen, Phys. Rev. A 22, 287 (1980); J. Stat. Phys. 27, 223 (1982).

⁴I. M. de Schepper, P. Verkerk, A. A. van Well, and L. A. de Graaf, Phys. Rev. Lett. 50, 974 (1983).

⁵A. A. van Well, P. Verkerk, and L. A. de Graaf, IRI Report No. 132-82-07 (unpublished) (available on request).

⁶J. Rouch, J. P. Boon, and P. A. Fleury, Physica A 88, 347 (1977).

⁷H. J. Maris, Rev. Mod. Phys. 49, 341 (1977).

⁸J.-B. Suck, H. Rudin, H.-J. Güntherodt, and H. Beck, Phys. Rev. Lett. 50, 49 (1983).

⁹O. Söderström, Phys. Rev. A 23, 785 (1981).